Journal of Magnetic Resonance **146,** 369–374 (2000)
doi:10.1006/jmre.2000.2178, available online at http://www.idealibrary.com on IDEAL®

Simultaneous Soft Pulses Applied at Nearby Frequencies

Matthias Steffen,*,† Lieven M. K. Vandersypen,*,† and Isaac L. Chuang†

*Solid State and Photonics Laboratory, Stanford University, Stanford, California 94305-4075; and
†IBM Almaden Research Center, San Jose, California 95120

Received April 19, 2000; revised July 24, 2000

The rotation of a spin subject to an on-resonance soft pulse and simultaneously to a soft pulse at a nearby frequency may strongly deviate from the desired rotation expected for a single on-resonance pulse. The deviation is the result of transient frequency shifts of the spin caused by the off-resonance irradiation. We show that the resulting error can be corrected by shifting the frequency of the on-resonance pulse in such a way that it tracks the shift of the spin frequency. Experimentally, the effectiveness of this simple and intuitive method is demonstrated for simultaneous inversions at nearby frequencies in the case of both coupled and uncoupled spins. Simulations predict that the correction technique is effective for arbitrary pulse shapes and tip angles and is particularly useful when the frequency window of the shaped pulse is two to eight times the frequency separation between the chemical shifts of the two spins.

Key Words: **simultaneous soft pulses; shaped pulses; Bloch–Siegert shift; Berry's phase.**

Many high-resolution NMR experiments (*1*), including NMR quantum computing experiments (*2, 3*), would benefit from the use of two or more simultaneous soft radiofrequency pulses. Soft pulses are designed to excite or invert spins over a limited frequency region, while minimizing x and y rotations for spins outside this region (*1*). However, soft pulses do cause z-rotations well outside the frequency window (*4*). This z-rotation is the result of a shift $\Delta\Omega_{\mathrm{BS}}$ in the spin precession frequency during irradiation at a nearby frequency. This effect has become known as a transient (generalized) Bloch–Siegert shift (*4–6*); at a deeper level, the acquired phase can be understood as an instance of Berry's phase (*7, 8*). The magnitude of $\Delta\Omega_{\mathrm{BS}}$ is approximately $\omega_1^2/2\Omega$ (for $\omega_1 \ll \Omega$), where ω_1 is the RF field strength and Ω is the frequency separation between the Larmour frequency of the spin in the absence of RF fields and the frequency of the RF field. The frequency shifts can easily reach several hundred hertz and the direction of the shift is always away from the frequency of the RF field.

Thus, when spin-selective pulses are applied simultaneously to two spins a and b with resonance frequencies ω_a and ω_b ($\omega_a < \omega_b$), the pulse at ω_a temporarily shifts the frequency of spin b to $\omega_b + \Delta\Omega_{\mathrm{BS}}$. As a result, the pulse on spin b, which is still applied at ω_b, will be off-resonance by an amount $-\Delta\Omega_{\mathrm{BS}}$. Analogously, the pulse at ω_a is now off the a-resonance by $\Delta\Omega_{\mathrm{BS}}$. The resulting rotations of the spins deviate significantly from the desired rotations. Figure 1 shows the simulated inversion profiles for a spin subject to two simultaneous Hermite 180° pulses (*9*) separated by 3273 Hz. The centers of the inversion profiles have shifted in frequency and the inversion is incomplete, which can be seen most clearly from the substantial residual xy-magnetization (>30%) over the whole region intended to be inverted. Note that since the frequencies of the applied pulses are off the spin resonance frequencies, perfect rotations cannot be achieved regardless of the tip angle settings.

Previous work (*10*) addressing this problem suggested the use of additional soft pulses to cancel out the frequency shifts of the spins. However, the extra pulses may have undesired effects on other spins in the spectrum. Another approach (*11*) is to time-reverse one of the two pulses, but this technique is not applicable for time-symmetric pulses and furthermore, the time-reversal introduces a frequency-dependent phase shift of the corresponding spin. A last method involves the brute-force optimization of the pulse shapes for simultaneous pulses (*12*). While this method yields pulse shapes capable of properly rotating spins close in frequency, it is mostly used in imaging experiments and has not found the same degree of application in the NMR community, which has continued to use standard pulse shapes. In practice, closely spaced simultaneous soft pulses have usually been avoided in NMR (*13*) or the poor quality of the spin rotations was accepted.

In this paper, we present an effective, intuitive, albeit simple alternative to the brute force optimization schemes. We show that the rotations of the spins can be significantly improved simply by shifting the carrier frequencies along with the shifts of the corresponding spin frequencies, such that at any given time, the pulses are applied on-resonance with the corresponding spin. Note that the magnitude of the frequency shift is generally not constant over the duration of the pulses so the RF frequency must vary accordingly. Yet, the calculation of the frequency shift throughout a soft pulse is straightforward and can be understood as follows. A shaped pulse is modeled (and in fact also implemented) as a sequences of time slices. The RF

1090-7807/00 $35.00

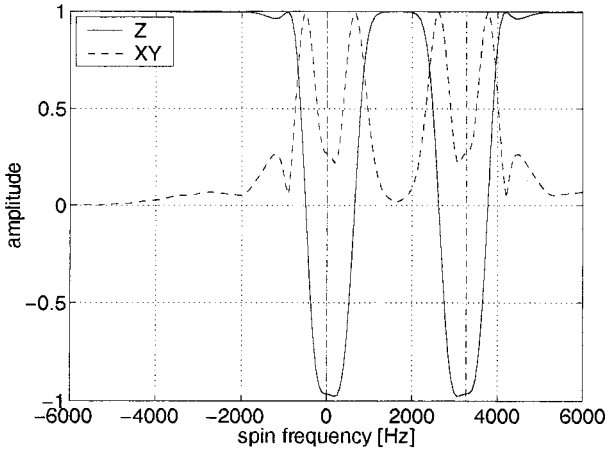

FIG. 1. Simulation of the amplitude of the z and xy component of the magnetization of a spin as a function of its frequency. The spin starts out along $+z$ and is subject to two simultaneous Hermitian-shaped pulses with carrier frequencies at 0 and 3273 Hz (vertical dashed lines), with a calibrated pulse length of 2650 μs (ideally 180°).

field has a constant amplitude and phase within each slice k, and the Hamiltonian governing the spin dynamics is thus also constant. The evolution of spin a during a *single* slice k of a shaped pulse at frequency ω_b can then be described by the 2×2 unitary operator

$$U_k^a = e^{-iH_{\mathrm{RF},k}^a \Delta t_k}, \qquad [1]$$

where Δt_k is the length of the slice, and the Hamiltonian in the rotating frame of spin a is

$$H_{\mathrm{RF},k}^a = \omega_{1,k}^b [X \cos(\phi_k^b) + Y \sin(\phi_k^b)], \qquad [2]$$

where $\omega_{1,k}^b$ is the RF field strength and ϕ_k^b is the sum of two terms: one is the phase appropriate to the pulse shape (usually 0° or 180°), and the other is a term linearly varying with time at a rate $\omega_b - \omega_a$ divided by the pulse length (in the frame of spin a, the pulse at ω_b rotates at $\omega_b - \omega_a$). X and Y are the angular momentum operators along the x and y axes, respectively. The *total* unitary operator for slices 1 through k is then

$$U_{\mathrm{T},k}^a = \prod_{i=1}^{k} U_i^a. \qquad [3]$$

The z-rotation acquired by spin a during the first k slices is given by

$$\phi_{\mathrm{BS},k}^a = \arg[U_{\mathrm{T},k}^a(1,1)] - \arg[U_{\mathrm{T},k}^a(2,2)], \qquad [4]$$

where (1, 1) and (2, 2) denote matrix elements of $U_{\mathrm{T},k}^a$. Since $H_{\mathrm{RF},k}^a$ is written in the rotating frame of spin a, ϕ_{BS}^a is caused purely by the RF irradiation. By definition, the z-rotation at the start of the first slice is $\phi_{\mathrm{BS},0}^a = 0$.

Now, for short Δt_k the frequency shift of spin a during slice k of the pulse at ω_b is well approximated by

$$\Delta\Omega_{\mathrm{BS},k}^a \approx \frac{\phi_{\mathrm{BS},k}^a - \phi_{\mathrm{BS},k-1}^a}{\Delta t_k}. \qquad [5]$$

It can be seen that when a second pulse is applied simultaneously, with a carrier frequency ω_a, the frequency of this pulse can be made to track the frequency shift of spin a slice-by-slice, simply by adding $\phi_{\mathrm{BS},k}^a$ to ϕ_k^a for each slice k (assuming for now that both pulses have the same duration and number of slices). The frequency shift of spin b during a pulse at ω_a can be calculated the same way and similarly, $\phi_{\mathrm{BS},k}^b$ must be added to ϕ_k^b.

Figure 2 shows the simulated inversion profiles for the same conditions as in Fig. 1, but this time using the frequency shift corrected scheme. The inversion profiles are almost perfect; there is very little (≈8%) leftover xy magnetization.

We simulated the inversion profiles for a variety of pulse widths and frequency separations, for hermite (*9*), gaussian (*14*) and REBURP (*15*) pulses. In all cases the improvements are impressive. Figures 3 and 4 show the inversion profiles for REBURP pulses without and with the correction scheme, respectively; the correction scheme reduced the residual xy magnetization from over 55% to less than 15%. The fact that even the delicate BURP class of pulses responds so well to this correction scheme illustrates the versatility and robustness of the technique.

Figure 5 shows the rotation angle (ideally 180°) of the spins as a function of the difference between ω_a and ω_b for two simultaneous Hermite pulses of a fixed pulse width, with and without the correction technique. Figure 6 is similar but in this

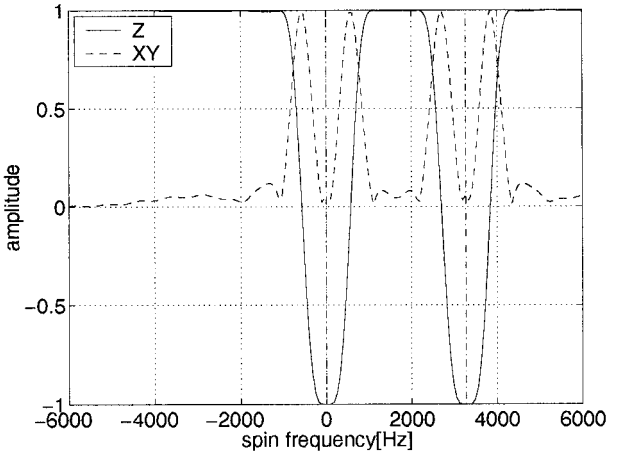

FIG. 2. Same as Fig. 1 but *with* the frequency shift correction.

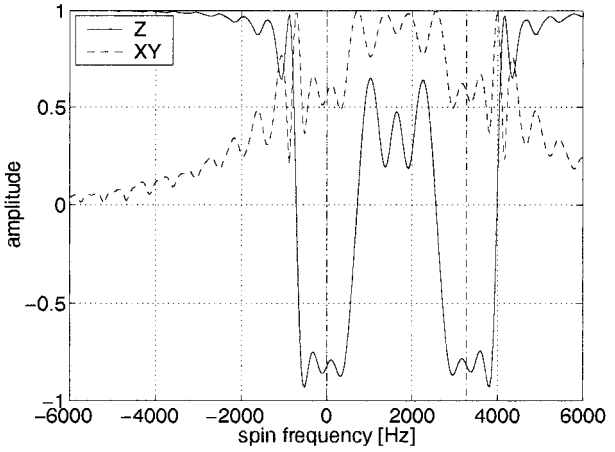

FIG. 3. Same as Fig. 1, i.e., no correction, but for 3800 μs REBURP pulses.

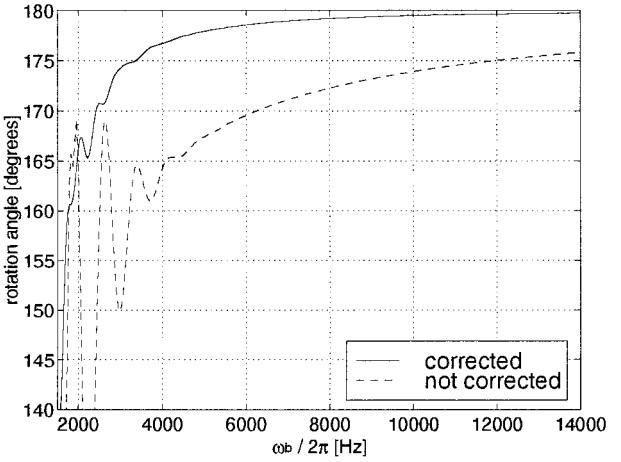

FIG. 5. Simulation of the rotation angle of a spin at 0 Hz after simultaneous Hermite pulses are applied at $\omega_a/2\pi = 0$ Hz and at $\omega_b/2\pi$ Hz, as a function of ω_b. The initial state of the spin was along z and for the calibrated 2650 μs pulse length; the rotation angle should ideally be 180°.

case simultaneous REBURP pulses were used. In both cases, the inversion bandwidth $\Delta\omega/2\pi$ is ≈1500 Hz (width of the profile at half height), as can be seen from Figs. 2 and 4. For the uncorrected Hermite pulses, the rotation angle error is below 5° only when $\omega_b - \omega_a > 2\pi$ 12,000 Hz $= 8\Delta\omega$. With the correction, this condition is relaxed to $\omega_b - \omega_a > 2\pi$ 3200 Hz $\approx 2\Delta\omega$. Similarly, for the REBURP pulses, the range where the rotation error is <5° is extended from $\omega_b - \omega_a > 2\pi$ 15,000 Hz $= 10\Delta\omega$ to $\omega_b - \omega_a > 2\pi$ 4500 Hz $= 3\Delta\omega$. In both cases, the rotation error is reduced by on average a factor of 8 over the range of $2\Delta\omega < \omega_b - \omega_a < 8\Delta\omega$, with a maximum reduction in the rotation angle error of more than a factor of 15.

We have experimentally confirmed the improvements predicted by the simulations, using a (50/50)% mixture of tetrafluoro-para-benzoquinone and tetrafluoro-teraphtalic acid. The ^{19}F spectrum consists of two singlets spaced by 6.96 ppm, corresponding to 3273 Hz at the 11.7 T field used in the experiments. Simultaneous 2650 μs (180°) Hermitian shaped pulses with 256 slices were created using only one channel of a Varian Unity Inova spectrometer equipped with waveform generators. The frequency was set on the resonance of one spin, while the other spin was addressed using phase-ramping techniques (*16*). Figure 7 illustrates the experimental improvements that can be achieved by shifting the carrier frequencies throughout the pulse duration. *Without* the correction, the left-over *xy* magnetization is about 30% of full strength. *With* the correction, the inversion is almost complete, with very little *xy* magnetization left. The results are in excellent qualitative and quantitative agreement with the simulations of Figs. 1 and 2.

So far, all the results have considered spins initially along $+z$. In order to apply the same rotation on an arbitrary input

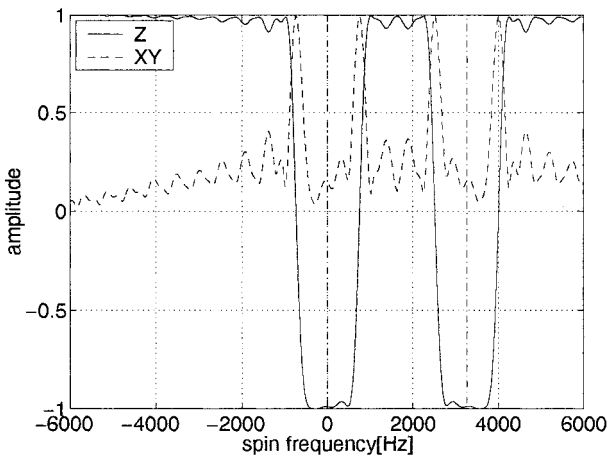

FIG. 4. Same as Fig. 3 but *with* the frequency shift correction.

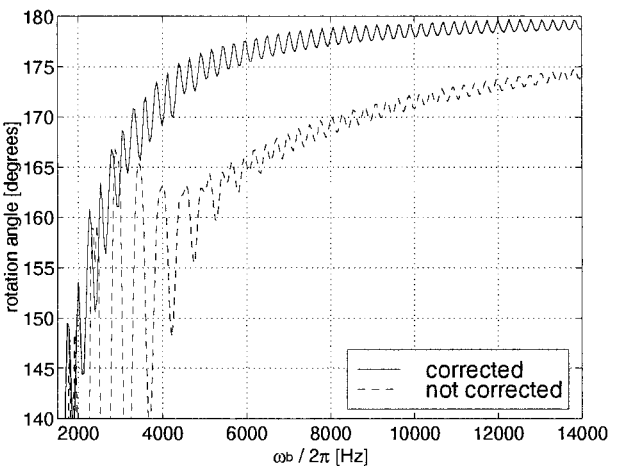

FIG. 6. Same as Fig. 5 but for simultaneous REBURP pulses (3800 μs).

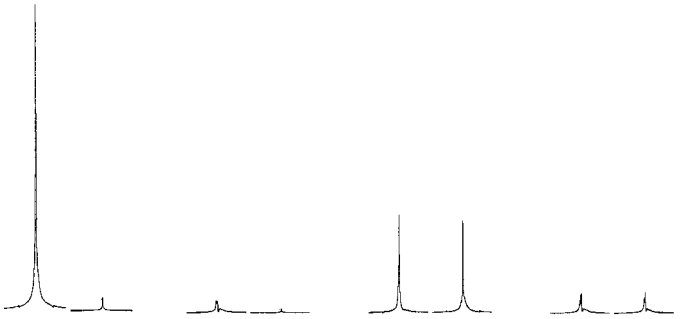

FIG. 7. The figure shows four pairs of experimentally measured spectra (absolute value); for each pair, the spectrum of spin *a* is on the left and the spectrum of spin *b* is on the right. The first pair was taken after a 90° Hermitian pulse on *a*, and the second pair was taken after a Hermitian 180° pulse on *a*. These serve as reference spectra. The third pair was taken after simultaneous Hermitian 180° pulses on the two spins *without* the correction scheme. The last pair is the same but *with* the correction scheme. The experimental parameters are the same as those used in the simulations of Figs. 1 and 2.

state, it is sufficient for the pulses to be time symmetric in the respective spin frames (*17*). Even though the pulse shapes we chose are universal (i.e., insensitive to the input state), it may appear that the time symmetry is lost by shifting the carrier frequency. However, the fact that this is not the case is a subtle point, which is clearly seen in the shifting spin frame as follows: when two pulses are close in frequency, the pulse at ω_b will shift the *resonance frequency* of spin *a* and vice versa. Since the spin frame is now shifting, a pulse at a fixed carrier frequency will not appear time-symmetric as seen by the spin. However, the asymmetries disappear and the pulse retains its original symmetry in the spin frame when the shift in resonance frequency is tracked and the pulse frequency adjusted accordingly.

Another way to analyze the universality of a rotation is to calculate the unitary matrix which contains all information about the rotation. The *ideal* unitary matrix for a 180° pulse about the *x* axis on any input state is given by

$$U_{\text{ideal}} = \begin{pmatrix} 0 & -i \\ -i & 0 \end{pmatrix}. \qquad [6]$$

The unitary matrix resulting from applying the pulses without any correction scheme (for the parameters of Fig. 1) is

$$U_{\text{uncorrected}} = \begin{pmatrix} 0.0119 - 0.1353i & -0.9907i \\ -0.9907i & 0.0119 - 0.1353i \end{pmatrix}. \qquad [7]$$

The unitary matrix obtained using the correction scheme (for the parameters of Fig. 2) is given by

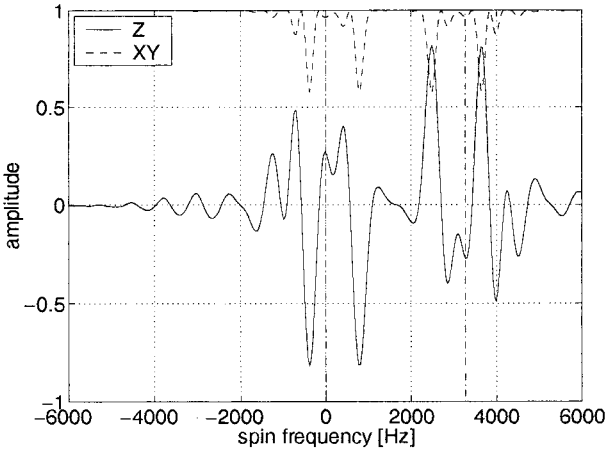

FIG. 8. Simulated excitation profile after a 90° pulse about $-y$ is applied followed by a 180° pulse about x, without using the correction scheme.

$$U_{\text{corrected}} = \begin{pmatrix} 0.0271 - 0.0045i & -0.9996i \\ -0.9996i & 0.0271 - 0.0045i \end{pmatrix}. \qquad [8]$$

Clearly, the unitary matrix obtained using the correction scheme approximates the ideal one much more closely than the uncorrected unitary operator. This means that the proposed correction scheme improves the rotations for any input state.

As an illustration, Figs. 8 and 9 show the excitation profiles of a spin initially along $-x$ followed by a 180° pulse about x without and with the correction scheme. Ideally, M_{xy} should be 1 at ω_a and ω_b while M_z should be zero. We further verified, using similar plots, that indeed any state initially in the xy plane subject to the 180° rotation (i.e., $U_{\text{corrected}}$ from Eq. [8]) reaches the desired final state.

Note that in practice the frequency synthesizer outputs a fixed carrier frequency. The frequency of the pulse is shifted by

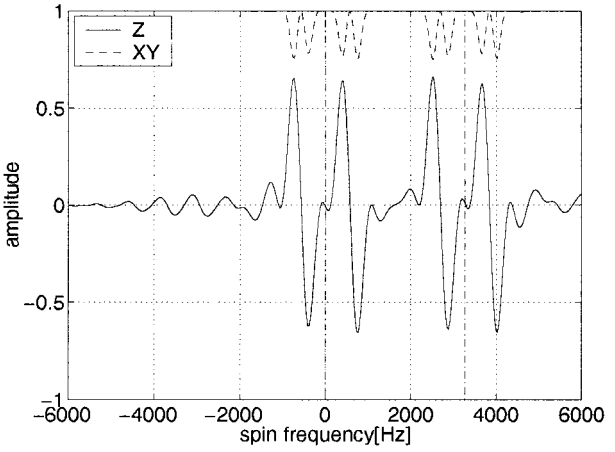

FIG. 9. Same as Fig. 8 but *with* the frequency shift correction.

modulating the phase of the carrier frequency. As a consequence, at the end of the pulse the spin frame and fixed reference frame of the carrier are rotated out of phase with respect to each other. In order to align the spin and references frames, a *z*-rotation needs to be applied. This can be done easily by adjusting the phases of all subsequent pulses on that spin. No extra effort is required to calculate the amount of *z*-rotation as it is simply given by Eq. [4] at the last slice, a calculation already performed when determining the frequency correction.

One might expect that coupling between the two spins involved would undermine the above technique (*11*), because the dynamics is now governed by a 4×4 unitary matrix rather than by a 2×2 unitary matrix. However, we demonstrated experimentally that this is not the case, at least not when $J \ll \omega_b - \omega_a$. Figure 10 shows a series of spectra analogous to that of Fig. 7 but this time the Hermite pulses were applied to coupled multiplets. Despite the fact that the coupling between the spins was ignored, a more than threefold reduction in the leftover *xy* magnetization is achieved using the correction scheme.

We verified by simulations that the same tools can be used to correct the frequency offsets caused by three or more simultaneous soft pulses at nearby frequencies. Similarly, the technique applies equally well to pulses for arbitrary tip angles. Furthermore, we made some minor extensions to the protocol presented above for calculating the phase corrections $\phi_{BS,k}$, to accommodate simultaneous pulses of different lengths. Finally, we tried to improve the inversion profiles even more using an iterative procedure. The idea is that the corrected pulses are shifted in frequency compared to the original pulses; hence one could take those improved pulses as the input of a second iteration of the correction scheme and iterate until the corrections converge. However, we found that little, if anything, is gained by such a procedure, in part because the results are already very good after the first iteration. Nonetheless, a slight increase in the amplitude of the pulses does make the rotation matrix more accurate (this was not done in the simulations and spectra shown above), especially when $\omega_b - \omega_a$ approaches the bandwidth $\Delta\omega$ of the pulse. Using the same settings as in Fig. 2, Fig. 11 shows the M_z magnetization component after the π pulse with and without the correction scheme as a function of tip angle. It can be clearly seen that slightly increasing the tip angle (about 2% in this case) even further improves the rotations. Increasing the tip angle without the correction scheme results in little gain for a wide range of settings. As the frequency separation decreases, larger increases in tip angle are needed for the M_z magnetization to be nearly -1. Further improvements beyond the frequency shift correction are thus clearly possible.

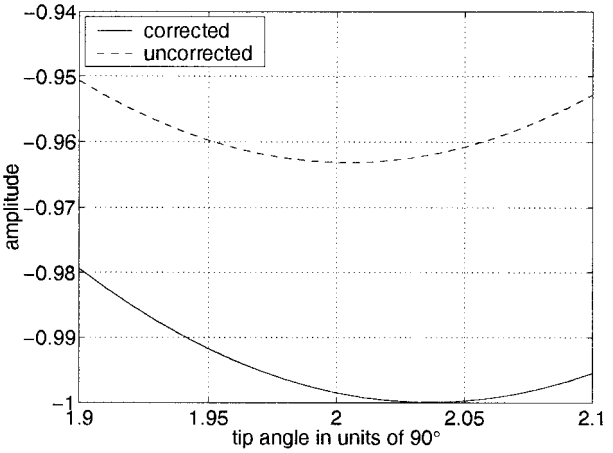

FIG. 11. Simulated amplitude of the M_z component as a function of the tip angle, with and without the correction using the same settings as in Fig. 2.

In summary, when several pulses are applied simultaneously at nearby frequencies, the rotations of the spins can be made as much as 15 times more accurate by ensuring that the carrier frequencies track the frequencies of the corresponding spins as they shift during the pulse execution. Computing the phase corrections for each slice is straightforward; no optimization or iteration is involved. This technique provides intuitive insight into the spin dynamics during the application of simultaneous pulses. Furthermore, it is an effective and fast alternative to the existing pulse optimization schemes, and could be easily incorporated into pulse shape design software.

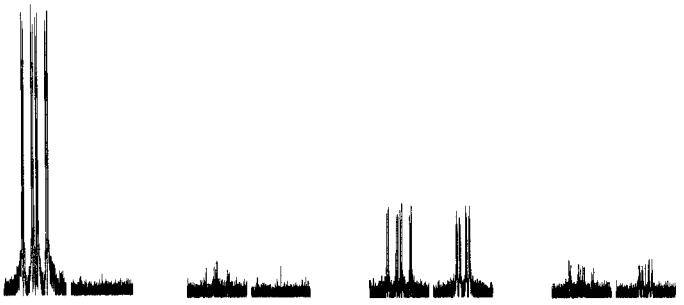

FIG. 10. A series of spectra analogous to that of Fig. 7 is shown. Hermitian-shaped pulses (1800 μs) were applied simultaneously to two multiplets 5389 Hz apart. The *J*-coupling between the two spins was 80 Hz.

ACKNOWLEDGMENTS

We thank Nino Yannoni for preparing the samples and for comments on the manuscript, Steve Smallcombe, Dwight Nishimura, and Ēriks Kupče for useful discussions, Anne Verhulst for comments on the manuscript, and James S. Harris and William Risk for support. L.V. gratefully acknowledges a Yansouni Family Stanford Graduate Fellowship. This work was supported by DARPA under the NMRQC initiative.

REFERENCES

1. R. Freeman, "Spin Choreography," Spektrum, Oxford (1997).
2. N. Gershenfeld and I. L. Chuang, *Science* **275,** 350 (1997).
3. D. G. Cory, A. F. Fahmy, and T. F. Havel, *Proc. Nat. Acad. Sci.* **94,** 1634 (1997).

4. L. Emsley and G. Bodenhausen, *Chem. Phys. Lett.* **168,** 297 (1990).
5. F. Bloch and A. Siegert, *Phys. Rev.* **57,** 522 (1940).
6. N. F. Ramsey, *Phys. Rev.* **100,** 1191 (1955).
7. G. B. Furman and I. M. Kadzhaya, *J. Magn. Reson. A* **105,** 7 (1993).
8. M. V. Berry, *Proc. R. Soc. London A* **392,** 45 (1984).
9. W. S. Warren, *J. Chem. Phys.* **81,** 5437 (1984).
10. M. A. McCoy and L. Mueller, *J. Magn. Reson. Ser. A* **101,** 122 (1993).
11. Ē. Kupče and R. Freeman, *J. Magn. Reson. A* **112,** 261 (1995).
12. J. Pauly, P. Le Roux, D. Nishimura, and A. Macovski, *IEEE Trans. Med. Imaging* **10,** 53 (1991).
13. N. Linden, Ē. Kupče, and R. Freeman, *Chem. Phys. Lett.* **311,** 312 (1999).
14. C. J. Bauer, R. Freeman, T. Frenkiel, J. Keeler, and A. J. Shaka, *J. Magn. Reson.* **58,** 442 (1984).
15. H. Geen and R. Freeman, *J. Magn. Reson.* **93,** 93 (1991).
16. S. L. Patt, *J. Magn. Reson.* **96,** 94 (1992).
17. J. T. Ngo and P. G. Morris, *J. Magn. Reson.* **74,** 122 (1987).